The Statistical Approach for Overcoming the Sensor Saturation Effect in Passive Ranging

S. T. Mitrovi [1], B. P. Bondžuli [1], M. S. Andri [1], Ž. P. Barbari [2]
[1]*University of Defence in Belgrade, Military Academy,*
Serbia
[2]*State University of Novi Pazar,*
Serbia
srdjan.mitrovic@va.mod.gov.rs

Abstract—Grey level intensity distribution on thermal infrared images is estimated in this research. General Pareto distribution describes grey level distribution better than other considered statistics. Error of passive ranging distance estimation based on intensity method is too large at short distance, because grey level of imaging sensor is saturated. Suggested modification has a great application in compensation of the effect of sensor saturation. Experiment on real saturated infrared sequence demonstrates that distance estimation error of suggested approach increases around three times slower compared to the conventional intensity based approach.

Index Terms—Infrared image sensors, image sequence analysis, grey level intensity, intensity saturation, parameter estimation, statistical analysis.

I. INTRODUCTION

Optical flow and stereo vision are the most common techniques used to passively estimate distance to an object. Both methods are relied on the geometrical principle of triangulation. In optical flow, the baseline is created due to the sensor motion, whereas in stereo the distance between cameras (baseline) is fixed [1]. Number of used sensors varies from one in optical flow method, through two for single baseline approach, to three or more for multiple baseline method and methods exploring the network of passive sensors. This research is focused on scenarios where only one passive imaging sensor is available.

A few different approaches for passive ranging using a single image sensor are known. The methods presented in [2] and [3] utilize size changes of a target in the image sequence to compute distance to the target. The approach for tracking emissive targets by a monocular passive sensor presented in [4] is based on atmospheric oxygen absorption in near-infrared spectrum, since research [5] utilizes spectral attenuation of two oxygen absorption bands in the visible and near-infrared spectrums for distance to target estimation.

In a recent research [6] two new passive ranging methods based on intensity and contrast measurements are proposed and compared with method based on object size

measurement in [7]. It is shown in [6] that error of distance estimation based on contrast method is less than that of the produced by size changes based method. Moreover, intensity based method produces even better results than contrast method. Real life application of distance estimation based on intensity measurements, using one [6] or more [8] passive sensors, is limited by characteristics of used sensors. The effect of sensor saturation has a significant influence on distance estimation accuracy at relatively short distances [6]–[9]. After extracting the target's pixels from the background, level of pixel intensity is bounded with threshold from one side. Maximal pixel intensity that can be measured causes another limit, known as sensor saturation.

Target tracking approach with two passive infrared sensors suggested in [8] cannot be used in cases where the distance between the sensors and the target is less than the value determined by the maximum output power of the sensors (saturation limit). It is well known that influence of sensor saturation effect increases as distance from the target to the sensor decreases. Research [9] overcomes saturation from atmospheric propagation model estimation by it fusion with object surface measurements and target motion analysis.

The main goal of this research is enhancement of distance estimation based on intensity measurements when sensor operates in saturation conditions. Relevant literature does not include many reports on the phenomenon of saturation using single sensor, such that this paper is deemed to be a modest contribution to the important field of passive ranging.

Since the distance estimation is based on target's intensity measurements, it is essential to determine intensity in both cases, normal conditions and sensors saturation. The first case is solved in [6], and this research addresses the second, more complicated case. It is expected that the mean target's intensity in the saturation can be estimated more correctly with suggested method based on object's statistics knowledge and relevant measurements in saturation than by conventional methods based on measurements.

Another important topic this research is deal with, is to find distribution fitting the target's statistic the best, and estimate their parameters in saturation. Using the Quantile-Quantile (QQ) plots of the real infrared video sequence of a

target, which is moving smoothly toward the sensor, the same statistical distribution of the target's pixels is verified before sensor saturation occurred. Eight commonly used statistical distributions are considered. Coefficient of linear correlation between real data quantiles and appropriate theoretical distribution quantiles on the QQ-plot is used as quality criterion for distribution fitting, and it is found that General Pareto (GP) distribution satisfied established criterion with the highest rank.

The GP distribution parameters can be determined by various methods [10], [11]. This research suggests a procedure for the estimation of GP distribution parameters, and an estimation of the average of the target's grey level in saturation. It is shown that, relying on target statistics in normal operation conditions and relevant measurements in saturation, significant improvement of distance estimation can be achieved. The quality of suggested method is tested on real infrared sequence, and a relative error of distance estimation in saturation is up to ten percent smaller than error of standard intensity approach.

The rest of paper is organized as follows. Section II describes the posed problem. Section III is dedicated to the QQ-plot analysis of the intensities of the target's pixels on a real infrared video sequence. Section IV deals with the choice of distribution fitting target statistics. The procedure for the estimation of GP distribution parameters; estimation of the average of the target's grey level in saturation and their verification through the experiment on real infrared sequence are described in Section V.

II. SENSOR SATURATION PROBLEM

The application of intensity based method on the real infrared sequence is studied. The sequence is recorded using the Dual Observer Passive Ranging System (DOPRS) that is designed for tracking a single airborne target. The system utilizes two thermal cameras and calculates distance by triangulation method.

In this research, sequence from one camera is used, while the distance obtained from the DOPRS is used as the reference distance in analysis and comparison of results. The reference distance to the target in the analysed image sequence is determined with an absolute error of less than five meters. Figure 1(a) shows the first, Fig. 1(c) the 150th and Fig. 1(e) the 350th frames of the analysed infrared sequence. Scene intensity in infrared image is represented on grayscale image among the 256 levels of grey. Target in Fig. 1(e) has a significant amount of white pixels, indicating the saturation of the sensor.

The original approach suggested in [6] does not produce acceptable distance estimation when target is close to the sensor as a consequence of target intensity saturation. Probability of the target pixels intensity in the ith frame is defined as

$$\mathbf{p}_{(i)} = \frac{\mathbf{G}_{(i)}}{\sum_{k=0}^{255} \mathbf{G}_{(i)}(k)}, \qquad (1)$$

where $i = 1, 2, ..., N$, $\mathbf{G}_{(i)}$ denotes histogram of the target's

pixels intensity at the ith frame over the 256 bins and N is the total number of frames in the sequence. The threshold-„ for the detection and segmentation of the object in all frames is determined by the method of Tsai [12]. The results of detection and segmentation in first, 150th and 350th frames are shown in Fig. 1(b), Fig. 1(d) and Fig. 1(f), respectively.
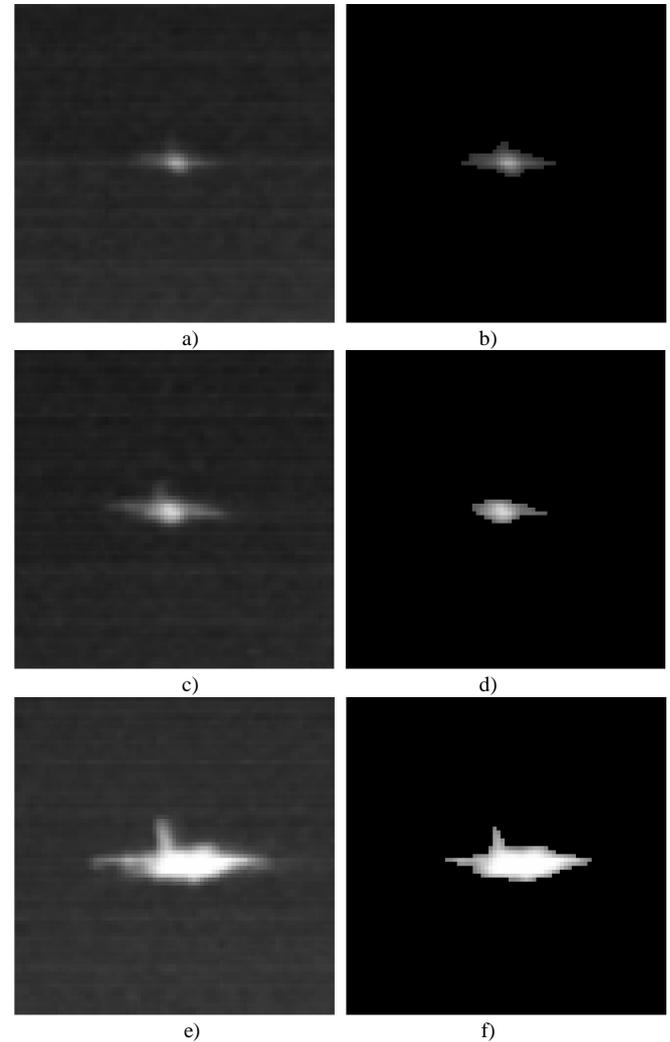

Fig. 1. Target in: a) the first, c) the 150th and e) the 350th frames in IR sequence. Target after detection and segmentation in: b) the first, d) the 150th and f) the 350th frames.
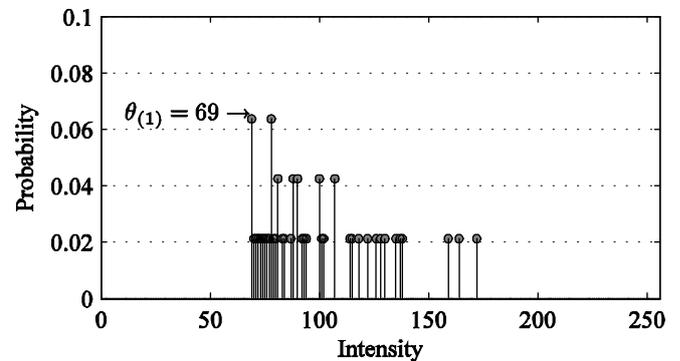

Fig. 2. Probability $\mathbf{p}_{(1)}$ of the target pixels intensity of the first frame.

Figure 2 shows probability of target pixel intensity (1) as a function of the intensity level in the first frame of the analysed sequence. It may be noted that the vector $\mathbf{p}_{(1)}$ is equal to zero when the pixel intensity is less than 69, which is the threshold value for the current frame ($_{„(1)} = 69$).

Figure 3 presents the results of the applying (1) on the 350th frame. In addition to $\mathbf{p}_{(350)}$ values are zero when pixel intensity is less than 136 ($_n{}_{(350)}$ = 136), a high value of probability can be noted at the upper limit of the range, as a result of saturation of the sensor.

The result of applying (1) to the whole sequence of images is a probability matrix

$$\mathbf{P_T} = \left[\mathbf{p}_{(1)}^T, \mathbf{p}_{(2)}^T, ..., \mathbf{p}_{(N-1)}^T, \mathbf{p}_{(N)}^T \right], \qquad (2)$$

which means that the matrix $\mathbf{P_T}$ size is $256 \times N$. The matrix $\mathbf{P_T}$ is illustrated in Fig. 4, and it can be noted that threshold parameter increases from the first frame ($_n{}_{(1)}$ = 69) to the 350th frame ($_n{}_{(350)}$ = 136), and high probabilities in matrix $\mathbf{P_T}$ (bright pixels in Fig. 4) move from the lower limit of the range (Fig. 2) to the upper limit of the range (Fig. 3). Saturation becomes dominant after the 300th frame, meaning that intensity of more than 20 percent of the target's pixel (white color on $\mathbf{p}_{(i)}$ = 255) is measured as upper sensor limit.
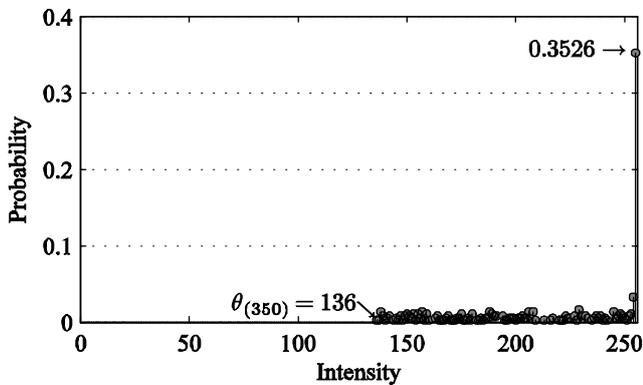

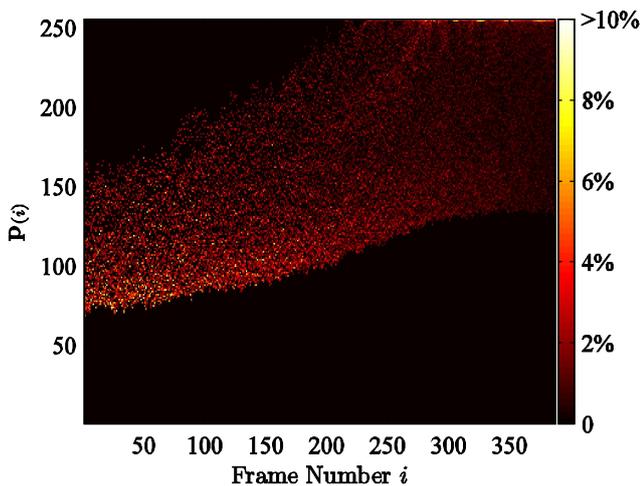Fig. 3. Probability $\mathbf{p}_{(350)}$ of the target pixels intensity of the 350th frame.

Fig. 4. Probability matrix $\mathbf{P_T}$ of the target pixels intensity in the sequence.

III. QQ-PLOT SEQUENCE ANALYSIS

It is assumed that the mean target's intensity in the saturation can be estimated on the basis of object's statistics. As one target is in the sequence, it is expected that its intensity has the same distribution function in the entire sequence, since the parameters of this distribution can change from frame to frame. 199 QQ-plots from analysed IR sequence of the target pixels intensities from the frame (i)

versus intensities from the frame (i-1) are shown in Fig. 5, where i takes values from 2 to 200. The short review of the QQ-plot technique is presented in [13].

It can be seen that most of the quantiles are close to the straight line of constant slope (45°) throwing the coordinate origin, indicating the same distribution of target intensity over the sequence [13]. Deviations from this line imply that the distribution parameters are changing with time of sequence, as expected with regard to the target's intensity levels shown in Fig. 4.

IV. TARGET'S INTENSITY DISTRIBUTION CONSIDERATION

It is assumed that the distribution of the intensity levels of the target can be described using one of the following distributions:
  - Weibull distribution;
  - Birnbaum-Saunders (BS) distribution;
  - Gaussian distribution;
  - Gamma distribution;
  - Nakagami distribution;
  - Lognormal distribution;
  - Inverse Gaussian distribution;
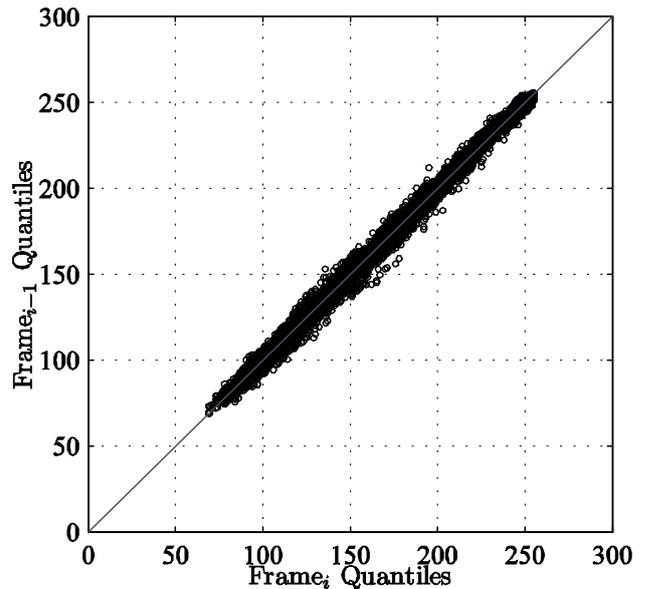 - General Pareto (GP) distribution [10], [11].

Fig. 5. QQ-plots of the target pixels intensities through the whole IR sequence, $i \in \{1, 2, ..., 200\}$.

The real data are fitted on the above distributions using maximum likelihood method, and as a result two parameters, describing appropriate distribution, are obtained for each sequence frame. With the aim of selecting which of the distributions best fits the real data, the following procedure is performed:

- QQ-plots of the analysed theoretical distribution against the real data is done, for first N=200 frames in the video sequence.

- Linear correlation coefficients r_i ($i = 1,2,...,N$) of points in QQ-plot are calculated, for all N = 200 frames.

- Mean value – $\overline{r}_{1:N}$ of all N = 200 linear correlation coefficients for analysed distributions is calculated.

Results of analyses are presented in Table I.

TABLE I. DISTRIBUTION FITTING RESULTS.

Distribution	$\overline{r}_{1:N}$	Rank
Weibull	0.95177	8
Birnbaum-Saunders (BS)	0.97580	2
Gaussian	0.95205	7
gamma	0.97261	5
Nakagami	0.96645	6
lognormal	0.97485	4
inverse Gaussian	0.97579	3
general Pareto (GP)	0.99371	1

On the basis of the given results it can be concluded that GP distribution the most closely describes the target's intensity for established criterion: mean value of linear correlation coefficients for analysed two hundred frames is the largest: $\overline{r}_{1:N} = 0.9937$. As an example, Fig. 6 and Fig. 7. show a QQ-plots of real data quantiles from one frame versus theoretically quantiles of GP (the first ranked) and BS (the second ranked) distributions, respectively, where straight lines represent a perfect match to distributions. The QQ-plot in Fig. 6 approximately matches the straight line, while in Fig. 7 deviations from the line are significant, which is an additional confirmation of the correctness of the distribution function choice.
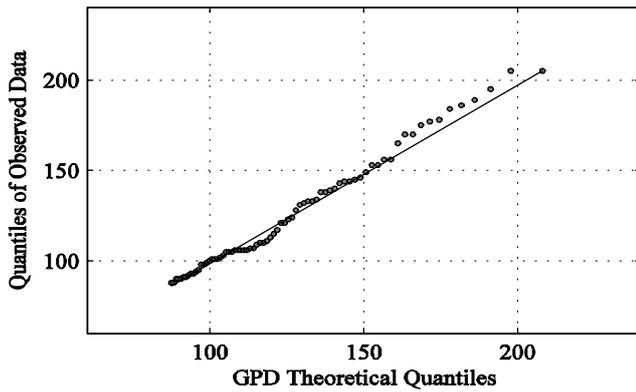

Fig. 6. The QQ-plot of the GPD theoretical quantiles versus real data quantiles.
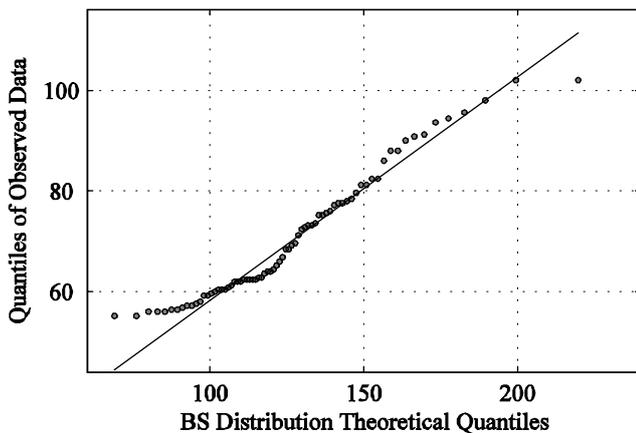

Fig. 7. The QQ-plot of the BS distribution theoretical quantiles versus real data quantiles.

V. EXPERIMENTAL RESULTS

Having previously established that the distribution of target's pixel intensity has a GP distribution, the distance to the target in saturation will indirectly be estimated on the basis of estimations of the shape parameter k and scale

parameter σ of the GP distribution (Appendix A), and the measured values of the threshold μ. It is assumed that the sensor saturation occurs when more than 20 % of the target's pixels have a maximum pixel intensity level, which in the analysed sequence occurs after 289 frames. The GP distribution parameters k and σ can be determined by various methods [10], [11], depending on their range. The ranges of estimated parameters are: $k \in [-1.4, -0.06]$, $\sigma \in [31, 180]$ and $\mu \in [68, 139]$. Since the relevant literature utilizes two different notations for the cumulative general Pareto distribution (GPD) function (sign of the shape parameter), notation used through this research is given in the Appendix A.

In [6] to estimate the distance to the target, average of the target's grey level (intensity) is used. In order to preserve information about the intensity mean it is more convenient to use the method of moments (MOM) instead of the maximum likelihood method to estimate parameters of the GP distribution. Figure 8 shows estimation of shape parameter $\hat{k}$ to the frame when sensor enters the saturation (grey circles). Parameter $\hat{k}$ data are fitted as a linear polynomial function based on estimations before the sensor saturation arises, and as a result, prediction $\hat{k}^P$ is obtained (full line), with the determination coefficient $r_{\hat{k}}^2 = 0.79$.

Estimations of scale parameter σ before sensor saturation are shown with grey circles in Fig. 9. Parameter σ data are fitted as a quadratic polynomial function based on estimations before the saturation occurred, and prediction σ^P of scale parameter is obtained as a result (full line), with the determination coefficient $r_\sigma^2 = 0.96$.

According to [6], the distance to the target in i^{th} frame is

$$D_{(i)} = D_{(i-1)} + \frac{1}{g} \ln \frac{I_{(i-1)}}{I_{(i)}}, \tag{3}$$

where $D_{(i)}$ and $D_{(i-1)}$ are distances from the object to the sensor, and $I_{(i)}$ and $I_{(i-1)}$ are the average grey levels of the object on two successive frames. Initial range $D_{(1)}$ and a reliable estimate of extinction coefficient are required. For this experiment, coefficient is estimated on the test sequence preceding the analysed, as suggested in [6], while initial distance $D_{(1)}$ is taken from DOPRS. Intensity of the target is presented in Fig 10. Grey line denotes intensity measured directly from the sequence denoted with $\overline{x}$, while black line identifies intensity estimation based on target statistics (Appendix A)

$$\hat{I}_{(i)} = \frac{\sigma_{(i)}}{1 - k_{(i)}} + \mu_i, \quad \begin{cases} \sigma_{(i)} = \hat{\sigma}_{(i)}, & k_{(i)} = \hat{k}_{(i)}, \quad i < i_{sat}, \\ \sigma_{(i)} = \hat{\sigma}_{(i)}^P, & k_{(i)} = \hat{k}_{(i)}^P, \quad i \geq i_{sat}, \end{cases} \tag{4}$$

where i_{sat} represents ordinal number of the frame at the time when saturation is detected.

It can be noted that before the saturation occurred, estimated intensity $\hat{I}$ had a good fit to the measured intensity $\overline{x}$, since the estimation of $\hat{I}$ is performed on the basis of

mean and variance of a real signal. In saturation $\hat{I}$ and $\bar{x}$ diverge, as expected. Distances to the target in the analysed sequence are calculated based on (3) and intensities $\hat{I}$ and $\bar{x}$, and results with a true distance from DOPRS are shown in Fig. 11. Distance $D_{(1)}$ from the DOPRS is used for initialization of (3) in both calculations.
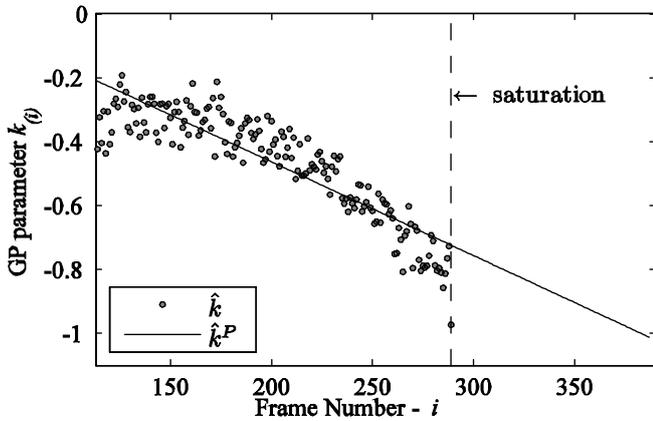

Fig. 8. Shape parameter of the GP target distribution, $\hat{k}$ -MOM estimated values, $\hat{k}^P$ -prediction in saturation conditions.
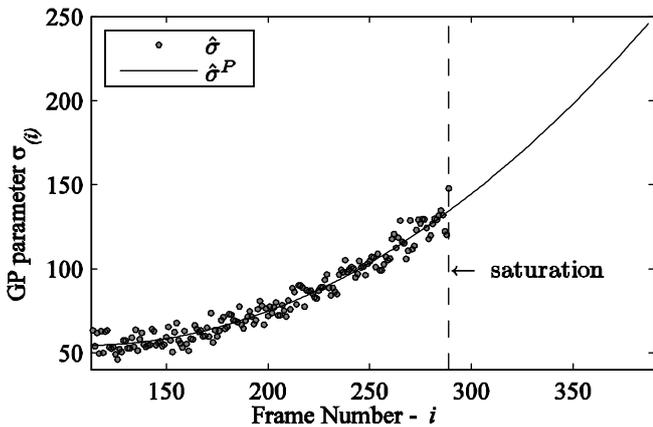

Fig. 9. Scale parameter $\hat{\sigma}$ of the GP target distribution, $\hat{\sigma}$ - MOM estimated values, $\hat{\sigma}^P$ - prediction in saturation conditions.
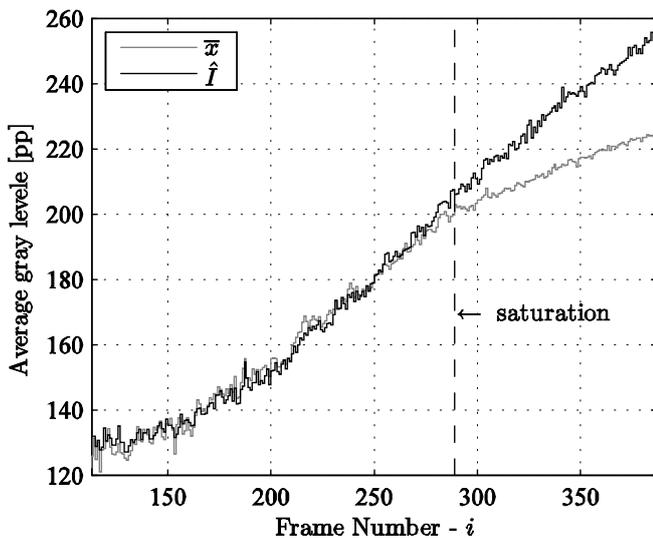

Fig. 10. Intensity of the target: grey line – direct measurements from the sequence; black line – calculated values based on GP estimated shape and scale parameters, and determined threshold.

Relative errors of distance estimation obtained by original

approach [6] and suggested modification are shown in Fig. 12. Significant improvement of distance estimation is clearly observable in saturated region (right side in Fig. 12.). Distance estimation error of GP based approach increases around three times slower compared to the conventional intensity based approach. This confirms the assumption that the distance to the target in the saturation can be estimated more accurately based on determined object's statistics and relevant measurements in saturation than by conventional method [6] based on raw measurements.
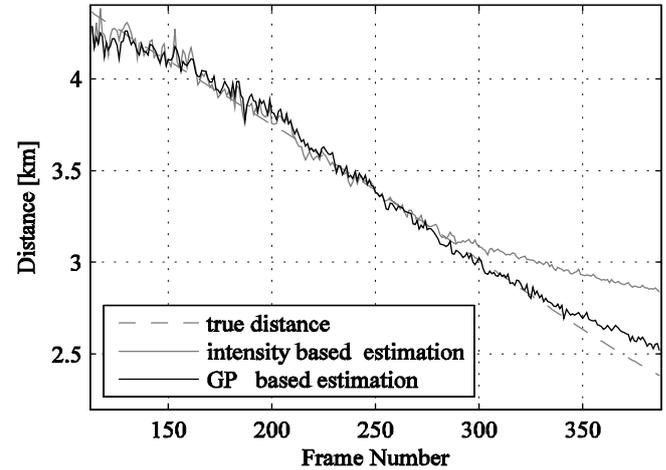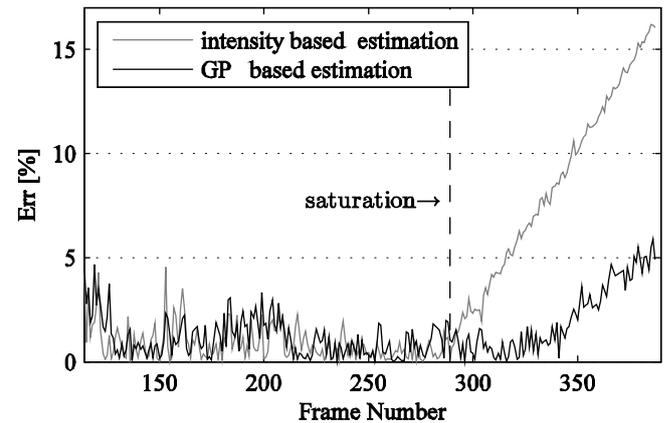

Fig. 11. True and estimated distances.

Fig. 12. Relative errors of distances estimations in the sequence.

VI. CONCLUSIONS

In authors' recent research [6], two new passive ranging methods based on intensity and contrast measurements are proposed and compared with the method based on object size measurements. It is shown that error of distance estimation based on contrast method is less than that of the produced by the size changes based method. Moreover, intensity based method produces even better results than contrast method. Error of passive ranging distance estimation based on intensity method is unacceptably large at short distances, since grey level of acquisition sensor is saturated.

This research suggests the extension of the intensity method for passive ranging using a single camera operating in normal and saturation conditions, enabling the significantly better distance estimation at short ranges. Estimation of the target's mean value of grey level in non-ideal conditions (sensor saturation) is based both on

evaluation of object statistics and image measurements, instead of using the only image measurements in standard intensity based approaches. It is found that general Pareto distribution is fitting real target intensity best, compared to other distributions analysed in the paper. A simple algorithm for GP parameters estimation and prediction is suggested and experimentally confirmed.

Experiment on real saturated infrared sequence verifies that a relative error of distance estimation is up to ten percent smaller and increases around three times slower compared to error of the conventional intensity based approach. Although the distance estimation error increases with intensity saturation time, the new approach enables additional time for target tracking, depending on its speed and size as well as of used image sensor characteristics.

APPENDIX A

Let X be a random variable. The cumulative GPD function with location, shape, and scale parameters $\mu \,(\mu \in \mathbb{R})$, $k(k \in \mathbb{R})$ and $\dagger \,(\dagger > 0)$, respectively, is defined as

$$F(x \mid \mu, k, \dagger) = 1 - \left(1 + k \frac{x - \mu}{\dagger}\right)^{-\frac{1}{k}}, \qquad (5)$$

where $k \neq 0$ and probability density function for the three parameters generalized Pareto distribution is

$$f(x \mid \mu, k, \dagger) = \frac{1}{\dagger}\left(1 + k \frac{x - \mu}{\dagger}\right)^{-\frac{k+1}{k}}. \qquad (6)$$

In applications when threshold parameter μ is known, its subtraction from signal X allows the use of two parameters GPD ($\mu = 0$), then (5) becomes

$$F(x \mid k, \dagger) = 1 - \left(1 + k \frac{x}{\dagger}\right)^{-\frac{1}{k}}, \qquad (7)$$

where $k \neq 0$ and (6) transforms to

$$f(x \mid k, \dagger) = \frac{1}{\dagger}\left(1 + k \frac{x}{\dagger}\right)^{-\frac{k+1}{k}}. \qquad (8)$$

The mean value and the variance of GPD($k, \dagger$) have the following expressions

$$E(X) = \frac{\dagger}{1 - k}, \qquad (9)$$

where $k < 1$.

$$Var(X) = \frac{\dagger^2}{(1 - k)^2(1 - 2k)}, \qquad (10)$$

where $k < 0.5$, while the mean value of three parameters GPD($\mu, k, \dagger$) is

$$E(X) = \frac{\dagger}{1 - k} + \mu, \qquad (11)$$

where $k < 1$. The time-honoured and direct MOM is widely used for estimating the parameters of the two-parameters GP distribution [10]. The MOM estimates of parameters k and $\dagger$ are obtained from expressions for the mean (9) and the variance (10), as follows:

$$\hat{k} = \frac{1}{2}\left(1 - \frac{\bar{x}^2}{s^2}\right), \qquad (12)$$

$$\hat{\dagger} = \frac{\bar{x}}{2}\left(\frac{\bar{x}^2}{s^2} + 1\right), \qquad (13)$$

provided $k < 0.5$, where $\bar{x}$ and s^2 stand for the sample mean and the sample variance, respectively [10].

REFERENCES

[1] T. Surgailis, A. Valinevicius, V. Markevicius, D. Navikas, D. Andriukaitis. "Avoiding forward car collision using stereo vision system", *Elektronika ir elektrotechnika (Electronics and Electrical Engineering)*, vol. 18, no. 8, pp. 37–40, 2012.

[2] C. Raju, S. Zabuawala, S. Krishna, J. Yadegar, "A hybrid system for information fusion with application to passive ranging", in *Proc. of Int. Conf. on Image Processing, Computer Vision and Pattern Recognition*, 2007, pp. 402–406.

[3] D. R. Van Rheeden, "Passive range estimation using image size measurements," Feb. 2 1999. US Patent 5,867,256.

[4] J. R. Anderson, M. R. Hawks, K. C. Gross, G. P. Perram, "Flight test of an imaging O (Xb) monocular passive ranging instrument", in *Proc. of SPIE*, vol. 8020, 2011, pp. 802005–12. [Online]. Available: http://dx.doi.org/10.1117/12.883484

[5] R. A. Vincent, M. R. Hawks, "Passive ranging of dynamic rocket plumes using infrared and visible oxygen attenuation", in *Proc. of SPIE*, vol. 8052, 2011, pp. 80520D–16. [Online]. Available: http://dx.doi.org/10.1117/12.883470

[6] Z. P. Barbaric, B. P. Bondzulic, S. T. Mitrovic, "Passive ranging using image intensity and contrast measurements", *Electronics Letters*, vol. 48, no. 18, pp. 1122–1123, 2012. [Online]. Available: http://dx.doi.org/10.1049/el.2012.0632

[7] B. P. Bondzulic, S. T. Mitrovic, Z. P. Barbaric, M. S. Andric, "A comparative analysis of three monocular passive ranging methods on real infrared sequences", *Journal of Electrical Engineering*, vol. 64. no. 5, pp. 305–310, 2013. [Online]. Available: http://dx.doi.org/ 10.2478/jee-2013-0044

[8] Z. M. Durovic, B. D. Kovacevic, G. D. Dikic, "Target tracking with two passive infrared non-imaging sensors", *Signal Processing, IET*, vol. 3, no. 3, pp. 177–188, 2009. [Online]. Available: http://dx.doi.org/10.1049/iet-spr.2008.0068

[9] M. De Visser, P. B. W. Schwering, J. F. de Groot, E. A. Hendriks, "Passive ranging using an infrared search and track sensor", *Optical Engineering*, vol. 45, p. 026402, 2006. [Online]. Available: http://dx.doi.org/10.1117/1.2173948

[10] P. de Zea Bermudez, S. Kotz, "Parameter estimation of the generalized Pareto distribution-Part I", *Journal of Statistical Planning and Inference*, vol. 140, no. 6, pp. 1353–1373, 2010. [Online]. Available: http://dx.doi.org/10.1016/j.jspi.2008.11.019

[11] P. de Zea Bermudez, S. Kotz, "Parameter estimation of the generalized Pareto distribution-Part II", *Journal of Statistical Planning and Inference*, vol. 140, no. 6, pp. 1374–1388, 2010. [Online]. Available: http://dx.doi.org/10.1016/j.jspi.2008.11.020

[12] W. H. Tsai, "Moment-preserving thresholding: A new approach", *Computer Vision, Graphics, and Image Processing*, vol. 29, no. 3, pp. 377–393, Mar. 1985. [Online]. Available: http://dx.doi.org/10.1016/0734-189X(85)90133-1

[13] G. S. Kvascev, Z. M. Durovic, B. D. Kovacevic, "Adaptive recursive M-robust system parameter identification using the QQ-plot approach", *IET Control Theory and Applications*, vol. 5, no. 4, pp. 579–593, 2009. [Online]. Available: http://dx.doi.org/10.1049/ iet-cta.2009.0647